Anti-Cancer Drugs 1996, **7**, pp. 70–77

A topographic study on the distribution of cisplatin in xenografted tumors on nude mice

Anders Johnsson and Eva Cavallin-Ståhl
Department of Oncology, University Hospital, S-221 85 Lund, Sweden. Tel: (+46) 17 75 00; Fax: (+46) 14 73 27.

The intratumoral distribution of cisplatin was studied in terms of platinum concentrations in tissue pieces and immunohistochemically detected cisplatin–DNA adducts in xenografted tumors on nude mice. Heterogeneities in drug distribution were calculated as standard deviations and coefficients of variation. A three-dimensional image of adduct distribution was produced which showed regions with low adduct levels to be topographically connected also in three dimensions. A model was presented for investigating the potential influence of vascularization and cell proliferation on intratumoral adduct distribution by using different immunohistochemical stainings of parallel tissue sections. A weak but significant correlation was found between cisplatin–DNA adducts and proliferation, which might indicate that the drug uptake and adduct formation is increased in proliferating cells.

Key words: Adducts, cisplatin, intratumoral distribution, proliferation, vascularization.

Introduction

Cisplatin [*cis*-diammine-dichloro platinum (II)] is one of the most active chemotherapeutic agents used in clinical practice. The cytotoxic activity of cisplatin is thought to be mediated by formation of adducts with DNA.

Several methods are available for quantitation of cisplatin. Platinum concentrations can be measured with, for example, flameless absorption spectroscopy (FAAS).[1] The cisplatin–DNA adducts can be detected immunohistochemically by using antisera elicited against the adducts.[2,3] With this technique the cisplatin–DNA adducts are visualized on the cellular level, which makes this a suitable approach for topographic analysis of adduct distribution within different tissues.

Drug uptake and accumulation is an important determinant for tumor cell sensitivity and subsequently for response to cisplatin therapy.[4] Little is known about the distribution patterns of cisplatin within tumors *in vivo*. Heterogeneity in drug distribution, with some tumor cells receiving sublethal drug concentrations, is one possible cause of treatment failure. There are several potential reasons for intratumoral drug heterogeneity, of which variations in blood supply probably is an important one.

The level of cell proliferation may also play a role in tumor cell sensitivity. Proliferating cells are more susceptible for damage by cytotoxic agents, but whether the drug accumulation is higher in proliferating cells is unknown.

The purpose of this investigation was to describe the intratumoral topographic distribution of cisplatin, in terms of platinum concentrations and cisplatin–DNA adducts. We also present a model for investigating the potential influence of vascularization and cell proliferation on intratumoral adduct distribution by using different immunohistochemical stainings of parallel tissue sections.

Materials and methods

Animal model, treatment and tissue preparation

Nude (*nu/nu*) BALB/c mice with a cisplatin-sensitive xenografted squamous cell carcinoma cell line (ÅB) in its 125–143th passage were used.[5]

Mice (5–8 weeks old) were inoculated s.c. bilaterally in the flanks with tumor cells, thus inducing two tumors on each animal. Approximately 3 weeks later, they were injected i.p. with a single bolus dose of 15 mg/kg of cisplatin. One hour post-injection the animals were killed by cervical dislocation and the tumors were quickly removed. Experiment 1 included three mice with six tumors. The length and the width of the tumors were measured and the volumes were calculated:[6]

$$\text{Volume} = (\text{length} \times \text{width}^2)/2$$

This work was supported by grants from the Swedish Cancer Society, the Medical Faculty of Lund and the donation funds of the University Hospital of Lund.

Correspondence to A Johnsson

Each tumor was then divided into three to 13 pieces and stored at −70°C for later platinum analysis. In Experiments 2 and 3 with 11 tumors from seven mice, the tumors were frozen on dry ice and multiple 10 μm cryostat sections were prepared on poly-L-lysine-coated slides and stored at −70°C for later immunohistochemical studies. One of these tumors was subjected to sectioning of the whole tumor (Experiment 2). Every third slice was used, amounting to a total of 76 slices. They were mounted on 19 slides for immunohistochemical analysis of cisplatin–DNA adducts.

From each of the remaining 10 tumors three parallel sections were prepared as above from the central part for immunohistochemical analysis of cisplatin–DNA adducts, MIB-1 and factor VIII, respectively (Experiment 3). Two orthogonal diameters were measured on the slices and the volumes were calculated according to the formula above.

Platinum (Experiment 1)

Platinum was quantitated in tumor pieces with FAAS. Tissue digestion was performed as previously described.[3] Measurements were made with a Varian Spectra AA-40Z with Zeeman background correction.

Cisplatin–DNA adduct analysis (Experiments 2 and 3)

An immunohistochemical staining technique for visualization of cisplatin–DNA adducts was performed as previously described, using the NKI-A59 antiserum (gift from Drs den Engelse and Blommeart, Netherlands Cancer Institute, Amsterdam) elicited against cisplatin–DNA interaction products.[2,7] A brown nuclear staining reaction was developed by peroxidase–anti-peroxidase complex and diaminobenzidine. Methyl-green was used as nuclear counterstain. All slides in each experiment (Experiments 2 and 3) were stained in the same batch, to avoid the methodologic error due to inter-batch variation. The staining reaction was quantitated with the computerized image analyzer CAS 200 (Cell Analysis System, Elmhurst, IL), using a two-color mask image technique with the quantitative nuclear antigen (QNA) software package. With a × 40 objective lens, each microscopic field was 150 × 80 μm and consisted of 50–100 cells. Results of the measurements were given as 'percentage positive nuclear area' (PNA). This procedure has been described and evaluated in a previous report.[7] In Experiments 2 and 3, PNA values represent either single-field measurements or mean values of a slice. The heterogeneity between measured fields was given as the coefficient of variation (CV) by the image analyzer. Only areas with morphologically intact tumor cells were analyzed. Stromal cells and necrotic cells were not measured.

The cisplatin–DNA adduct staining in Experiment 3 was generally weak. In five of the tumors the staining intensity was too low to allow reliable measurements and they were excluded from further analysis. Thus, the results presented from Experiment 3 were based on the remaining five tumors.

Three-dimensional (3-D) imaging (Experiment 2)

In Experiment 2 in which a whole tumor was sectioned and stained for cisplatin–DNA adducts, 3-D images were produced and volumes were calculated by using the Treatment Management System (TMS; Helax AB, Uppsala, Sweden). The normal application for TMS is dose-planning or radiotherapy for cancer patients. Treatment plans are usually based on computerized tomography (CT) images, but data can also be entered into the system by a video camera, which was done in the present study. Every forth of the 76 slices stained for cisplatin–DNA adducts was scanned, thus making up a 3-D set of data with 19 parallel images representing the whole tumor. The outlines of the tumor were drawn in all slices. All slices were measured with regard to cisplatin–DNA adducts in tumor cells and the PNA values in different areas of each slice were noted. Areas with low (PNA < 20) adduct levels were marked on the TMS images. Volumes of the whole tumor and regions with low adduct levels were calculated.

Vascularization (Experiment 3)

Blood vessels were identified by an immunohistochemical staining against the von Willebrand factor (factor VIII), which recognizes endothelial cells.[8] The 10 μm thick cryostat sections were thawed and fixed for 30 s in 4% formaldehyde. Endogenous peroxidase was blocked with H_2O_2 in methanol for

30 min. The slides were treated with rabbit anti-human von Willebrand factor (Dako, Denmark) diluted 1:1000 in PBS at 4°C overnight, followed by treatment with an ABC (biotin–avidin) complex (Dako) and diamminobenzidine to visualize the endothelial cells. Mayer's hematoxillin was used as nuclear counterstain.

Cell proliferation (Experiment 3)

Cell proliferation was visualized with the monoclonal antibody MIB 1, that recognizes the KI-67 antigen, which is expressed during G_1 phase, increases during the cell cycle and declines after mitosis.[9] All slides were stained in the same batch. The 10 μm thick cryostat sections were thawed, treated in a citrate buffer in a microwave oven for 2 min at maximum power (960 W) and 2 min at low power (defrosting position). Endogenous peroxidase was blocked with H_2O_2 in methanol for 30 min. The slides were treated with MIB 1 antiserum (Immunotech, Marseille, France) diluted 1:100 in PBS for 90 min in room temperature. Immunoperoxidase detection was achieved by using a standard ABC (biotin–streptavidin) method (Dako) followed by diaminobenzidine. A counterstaining step with methyl-green was copied from the adduct staining protocol.[7]

The staining reaction was quantitated with the same image analysis technique as the cisplatin–DNA adducts.[7] Results from this analysis were presented in terms of PNA values, both from single-field measurements and as mean values of one slice from each tumor.

Correlation between vascularization and adducts (Experiment 3)

Large capillaries were detected on the slide stained for factor VIII and the corresponding areas were identified on the parallel section stained for adducts (Figure 1 A and B). The adducts were analyzed and the PNA values were sorted according to the distance from the capillaries into four groups: 0–150, 150–300, 300–350 and 450–600 μm, respectively. This procedure was repeated in the five tumors in Experiment 3. A total of 87 measurements in relation to 22 capillaries were performed.

Correlation between proliferation and adducts (Experiment 3)

The contour of each tumor was enlarged onto a paper sheet to facilitate the topographic orientation on the tumor slices. Firstly the adducts were measured in a randomly selected area and the PNA value was marked on the map. Then the corresponding area was identified on the MIB 1 stained slide (Figure 2A and B). The area was measured and the PNA value was marked on the map. On each tumor in Experiment 3, 10–15 areas were analyzed in this manner, to obtain a total of 57 pairs of single-field PNA values representing cisplatin–DNA adducts and proliferative activity, respectively.

Statistics

Variation in platinum concentrations and cisplatin–DNA adduct levels are expressed as standard devia-

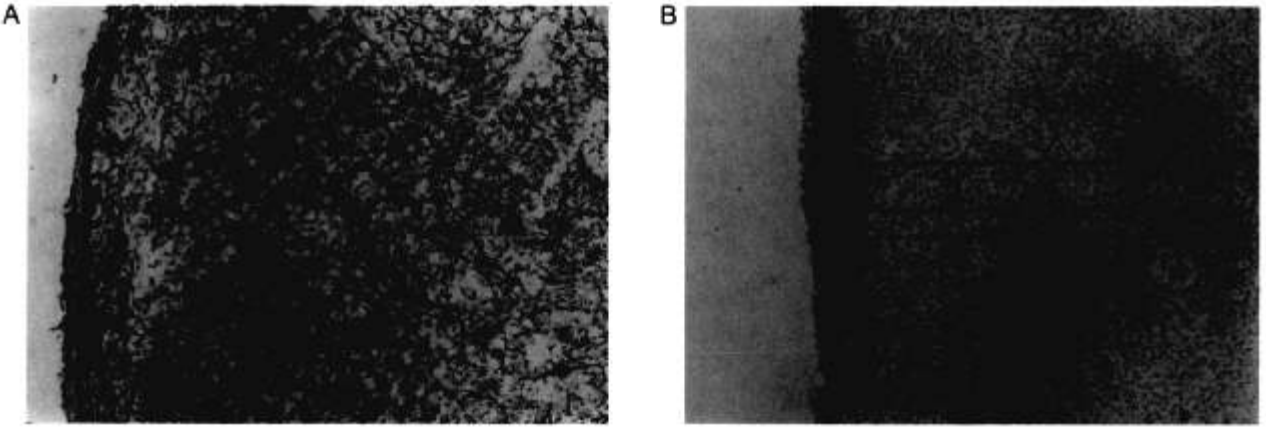

Figure 1. Microscopic images (10 × magnification) of parallel slices from a xenografted tumor from a nude mouse at 1 h after injection of 15 mg cisplatin/kg i.p., Experiment 3. (A) Factor VIII staining with brown endothelial cells. Arrow indicates large capillary. (B) Cisplatin–DNA adduct staining. Arrow indicates the same capillary as identified on (A). Rectangles represent areas measured for adduct levels at the four distance intervals from the capillary.

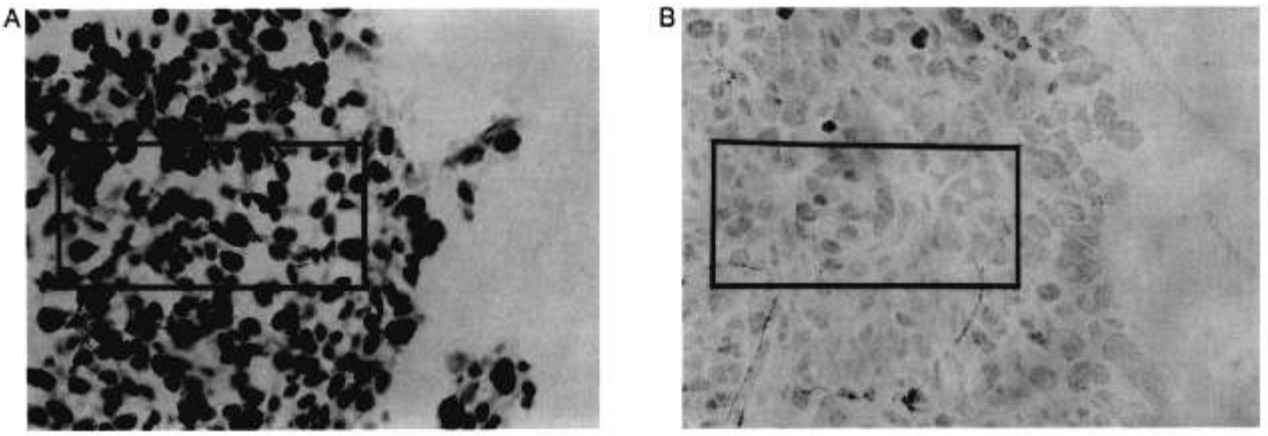

Figure 2. Microscopic images (40 × magnification) of parallel slices from a xenografted tumor from a nude mouse at 1 h after injection of 15 mg cisplatin/kg i.p., Experiment 3. (A) MIB 1 staining indicating cell proliferation. The rectangle represents a single-field measured. (B) Cisplatin–DNA adduct staining with a rectangle indicating the corresponding area as marked on (A), in which the adduct level was measured.

tions (SD) and relative standard deviations (coefficients of variation, CV). Correlations were calculated as Pearson's correlation coefficients (r). Comparisons of adduct levels between the four distances from large capillaries were made as paired t tests.

Results

Experiment 1

Platinum concentrations and intratumoral variations are shown in Figure 4. The mean platinum values for the six tumors ranged from 1.7 to 2.9 μg/g with SDs of 0.1–0.5 within the tumors and CVs were between

Figure 3. Three-dimensional image produced with TMS of a serially sectioned xenografted tumor from a nude mouse at 1 h after injection of 15 mg cisplatin/kg i.p., Experiment 2. The image consists of 19 slices stained for cisplatin–DNA adducts. The red lines indicate the outlines of the tumor and the pink lines are areas with low adduct levels (PNA < 20).

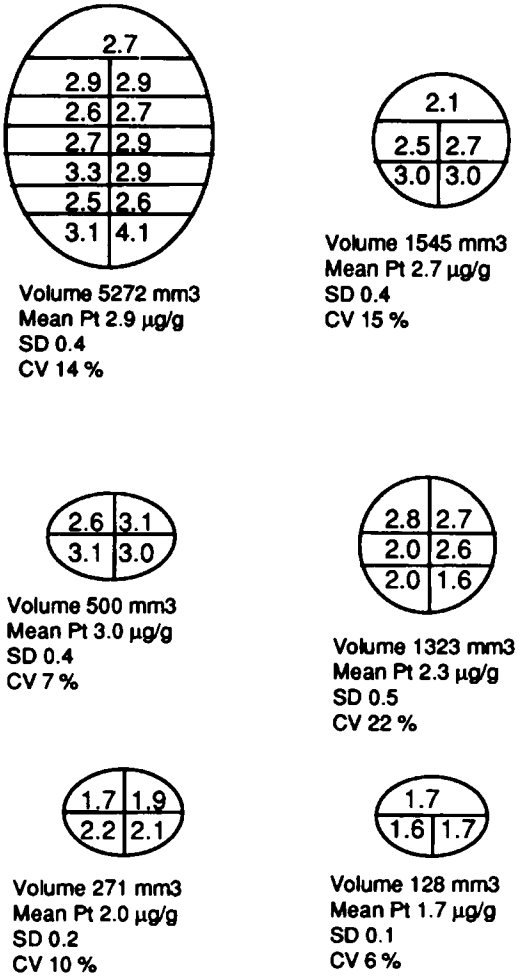

Figure 4. Platinum concentrations (μg/g) in six xenografted tumors from nude mice at 1 h after injection of 15 mg cisplatin/kg i.p. (Experiment 1). The tumors were divided into three to 13 pieces that were analyzed separately.

6% and 22%. There was a slight but not significant correlation between tumor volume and heterogeneity in platinum distribution, expressed as SDs ($r=0.56$, $p=0.24$) or CVs ($r=0.38$, $p=0.46$). The range of platinum concentrations within the tumors varied. In some of the tumors there was almost a 2-fold difference between the highest and lowest platinum levels.

Experiment 2

On the 76 serially sectioned tumor slices in Experiment 2, an average of 20 fields per slice were measured, representing a total of approximately 100 000 morphologically intact tumor cells. The intensity of the adduct staining was rather high with a mean PNA for the whole tumor of 28.6. The variation within the 76 slices had SD values ranging from 4.5 to 15.8 and CVs between 15 and 47%. The heterogeneity studied as comparisons between mean PNA values for each slice is seen in Figure 5. There was approximately a 2-fold difference between regions with high and low adduct levels.

Figure 3 shows a 3-D image of the whole tumor. The tumor volume as calculated in the TMS system was 32 mm^3. Areas with low (PNA < 20, approximately mean PNA − 2SD) adduct levels were also studied in three dimensions. This analysis revealed that the regions with low adduct levels were topographically connected also in three dimensions. The summarized volume of regions of tumor cells with a low adduct level was 1.6 mm^3 (5% of the whole tumor).

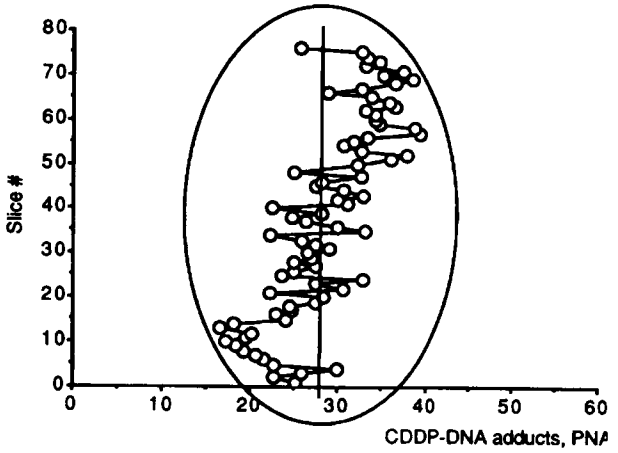

Figure 5. Cisplatin–DNA adducts in a xenografted tumor from a nude mouse at 1 h after injection of 15 mg cisplatin/kg i.p. (Experiment 2). The tumor was serially sectioned into 76 slices. The dots represent mean PNA (percentage positive nuclear area) values of each slice. The vertical line indicates the mean PNA for the whole tumor.

Experiment 3

On each of the five tumors, between 25 and 28 fields were measured, representing a total of approximately 2000 tumor cells per slice. The mean PNA values were between 6.3 and 16.3 (Table 1). The intratumor heterogeneity expressed as variations within slices had SDs ranging from 5.2 to 16.5 and the corresponding range of CV values was 75–119%.

There was no statistically significant correlation between tumor volume and heterogeneity in adduct distribution, in terms of SD values ($r=0.77$, $p=0.13$) or CV values ($r=0.35$, $p=0.57$).

All tumors were very well vacularized. Factor VIII-positive endothelial cells indicating capillaries, were seen mainly in the stromal parts of the tumor. Scattered endothelial cells were also seen within the tumor nodules (Figure 1A). The cisplatin–DNA adducts were analyzed in areas at different distances from large capillaries located in the stroma and the results are given as PNA values in Figure 6. There was a tendency for lower adduct levels closest to the large capillaries (0–150 μm) compared with tumor cells located farther away (150–600 μm) from the vessel.

The MIB 1 staining was very strong in all tumors (Figure 2A). On each slide 14–24 fields, representing a total of 1000–2000 cells per slice, were measured with image analysis. The staining was distributed fairly evenly on each slice, with CV values ranging from 7 to 16%. The 57 pairs of PNA values of adduct and MIB 1 stainings derived from corresponding areas on parallel slices were pooled together, and there was a weak but statistically significant correlation between MIB 1 and adduct levels ($r=0.37$, $p=0.004$) (see Figure 7). The cor-

Table 1. Cisplatin–DNA adducts in five xenografted tumors from nude mice at 1 h after injection of 15 mg cisplatin/kg i.p. (Experiment 3)

Tumor no.	Volume (mm^3)	No. of fields measured	Cisplatin		
			Mean PNA	SD	CV(%)
1	288	27	16.3	16.5	101
2	245	28	9.1	6.8	75
3	125	27	7.9	6.8	86
4	200	28	6.9	8.2	119
5	72	25	6.3	5.2	83

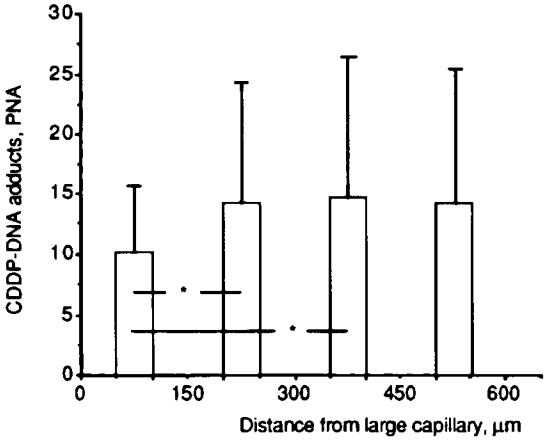

Figure 6. Cisplatin–DNA adducts at different distances from large capillaries in xenografted tumors from nude mice at 1 h after injection of 15 mg cisplatin/kg i.p. (Experiment 3). Parallel tissue sections were stained with Factor VIII to identify vessels and with NKI-A59 to visualize cisplatin–DNA adducts. Each bar indicates mean PNA and SD of 22 measurements ($p < 0.05$).

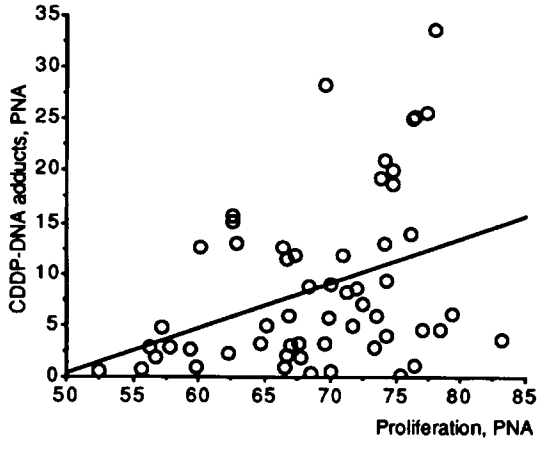

Figure 7. Correlation between cell proliferation and cisplatin–DNA adducts in 57 areas in five xenografted tumors from nude mice at 1 h after injection of 15 mg cisplatin/kg i.p. (Experiment 3). Parallel tissue sections were stained with MIB 1 to analyze cell proliferation and with NKI-A59 to visualize cisplatin–DNA adducts ($r = 0.37$, $p = 0.0042$).

relation between adducts and MIB 1 staining was also studied for each tumor separately, and positive correlation coefficients were found in all five tumors.

Discussion

This study describes the topographic distribution of cisplatin within tumors, using an *in vivo* model with xenografted squamous cell carcinoma on nude mice. We also present a method for exploring potential mechanisms for drug heterogeneities, by using different immunohistochemical stainings on parallel tissue sections.

There are many factors influencing the cytotoxic activity of cisplatin, e.g. drug accumulation, inactivation by glutathione and metallothionein, DNA repair, and tolerance for DNA damage.[4,10] Thus, drug uptake into the tumor cell is not the only determinant for cytotoxicity of cisplatin, but it is certainly a prerequisite for antitumor activity. *In vitro* studies often show correlations between cisplatin sensitivity and accumulation.[4] One potential reason for treatment failure with cisplatin is heterogeneities in drug distribution within the tumor, with some cells receiving sublethal intracellular concentrations of drug. This issue has only been sparsely addressed in the literature.

One of the objects with this study was to describe the drug distribution, in terms of platinum concentrations in tissue homogenates as well as cisplatin–DNA adducts analysis on immunohistochemically stained tissue slices. However, it is not evident how these heterogeneities should be described and quantitated. From a clinical point of view it would be of interest to identify regions in the tumors with sublethal drug concentrations and to distinguish tumor cells with very few adducts, since such cells possibly will escape chemotherapy-induced cell death and thereby prevent the tumor from being completely eradicated. The problem is that the 'lowest cytotoxic drug level' is not known, either for platinum concentrations nor for cisplatin–DNA adducts. Another disadvantage with this approach is that the 'lowest drug level' in a tumor is affected by the sample size. The more samples included in the analysis, the wider the range from minimum to maximum will be. Hence, in the absence of biologically relevant cut-offs and to avoid the influence of varying sample size in different tumors, we chose to express the intratumoral variations in terms of SD and CV values.

The distribution of platinum within tumors was fairly homogenous, with CV values ranging from 6% to 22%, at 1 h after a single i.p. injection of cisplatin. This was in accordance with a previous study on nude mice.[11] However the differences between the highest and lowest platinum concentrations varied by almost a factor 2 in some tumors, indicating that some areas did get clearly lower cisplatin exposure than others. A few clinical studies have shown considerable intratumoral variations in platinum concentrations in different portions of tumors at 2–3 weeks after cisplatin treatment. In a study by Richmond *et al.*[2] on patients with malignant fibrous histiocytoma there was a 2.6-fold average difference

between the highest and lowest platinum levels, and a mean intratumoral CV of 31%. Bielack *et al.*[13] studied platinum distribution in osteosarcoma and found a 'notable intratumoral variability' with platinum levels ranging from non-detectable (< 50 ng/g) to several hundred ng/g in the same tumor. Even though the studies are not really comparable, it appears that the heterogeneity in platinum distribution was lower in our study than in the above-mentioned clinical reports. This may be explained by differences in species, tumor type, tumor size or sampling time points.

Cisplatin is thought to exert its action by formation of adducts with DNA. Even though only a small portion, approximately 1%, of drug is bound to DNA[4] analysis of cisplatin–DNA adducts should be biologically more relevant than measuring total platinum in a tissue. However this remains to be shown. Topographic analysis of cisplatin–DNA adducts in tumors has not been published previously. In the present study cisplatin–DNA adducts were analyzed with immunohistochemistry, an approach that should be particularly apt for topographic studies. A disadvantage with all immunohistochemical assays is that the stoichiometric relations are incompletely known and therefore the results should be regarded as semi-quantitative rather than quantitative. There are also potential errors in the methodological procedure due to staining batch variations and observer variations in the image analysis.[7] The largest source of methodological error with the method is interbatch variation. Therefore all slides within Experiments 2 and 3, respectively, were stained in the same batch. The large difference in the overall staining level between slides in Experiments 2 and 3 illustrates this interbatch variation.

Adduct heterogeneity was also analyzed in three dimensions (3-D), by using the radiotherapy dose-planning system TMS in a somewhat unconventional way. We found this to be possible to perform, although it was very time consuming and therefore only one tumor was analyzed in this manner. Special interest was payed to areas with low staining level. This analysis showed that areas with low staining levels were connected also in 3-D, indicating that variations in staining on a slide do not appear by coincidence, which strengthens the validity of topographic analysis with this immunohistochemical method. The TMS can be used not only for production of 3-D images but also for calculation of volumes. The low adduct regions were entered manually into the TMS and should be regarded as approximated rather than precise areas. Therefore the volume calculated for low adduct regions should be interpreted as estimations and not exact volumes.

Were there any differences in heterogeneity between the distribution of adducts and platinum? This comparison is difficult for many reasons. Firstly, cisplatin–DNA adducts analyzed as staining intensity on immunohistological slides and platinum concentrations in μg/g homogenated tissue are not really comparable entities. Secondly, platinum measurements are quantitative whereas the adduct analysis is only semi-quantitative. Finally, the platinum heterogeneity studies were based on tissue pieces, whereas the adducts were analyzed on the microscopic level. The only adduct results that might be compared with the platinum data are the variation between mean PNAs of the multiple slices in Experiment 2, which yielded a 2-fold difference between regions with highest and lowest adduct levels. The platinum measurements in Experiment 1 showed an almost 2-fold difference between highest and lowest levels in some tumors. Thus, with all the limitations in mind, we could not find any obvious difference in heterogeneity between the platinum distribution and the adduct distribution.

Some potential reasons for heterogeneity in cisplatin distribution were also investigated. Tumor size did not correlate significantly with heterogeneity in the distribution of platinum or cisplatin–DNA adducts. However the comparisons gave positive correlation coefficients, and it is possible that investigation of a larger number of tumors would result in a statistically significant relation between tumor size and drug heterogeneity.

An adequate vascular system is required for sufficient drug delivery to the tumor cells. The tumors used in the present study were well vascularized. There was no obvious correlation between vascularization and tumor size. On the Factor VIII stained slides, large capillaries were seen mainly in the stroma, but scattered endothelial cells were also within tumor nodules, mixing with the tumor cells. To elucidate the mechanism of drug diffusion into the tumor the adduct levels were analyzed at different distances from large capillaries, with the hypothesis that the adduct levels should be higher in tumor cells close to the capillaries than further away. On the contrary, there was a tendency for lower adduct levels close to the capillaries. This could indicate that the scattered capillaries seen

among the tumor cells were capable of delivering drug to the tumor cells and that the capillaries that we chose to analyze were not crucial for drug delivery. It could also imply that cisplatin, being a small molecule, diffuses so easily into the tissue that the distance from the delivering capillary is of minor importance. The lack of correlation between adducts and distance from capillaries could also be due to the fact that the tumors were extremely well vascularized. Further studies should include tumors with a poorer blood supply.

Cell proliferation is an important determinant for cytotoxicity of cisplatin and most other anticancer agents. Cells in active cell cycle are more susceptible to damage by cisplatin than quiescent cells in G_0 phase. Whether proliferating cells also accumulate more drug and form more adducts is yet unknown. The MIB 1 staining gave very strong staining in all tumors, with low variation between and within tumors, indicating a very high proliferating activity. The low variation in MIB 1 staining decreased the possibilities to establish any strong correlations with the adduct staining levels. Nevertheless, there was a weak correlation between proliferation and adducts. This might suggest that uptake and adduct formation may be increased in more proliferating cells but the weakness in the correlation indicates that differences in proliferation could only account for a small part of adduct heterogeneity.

This investigation was performed on only one tumor cell line and with a limited number of tumors. Studies on other tumor types with larger variations in blood supply, cell proliferation and cisplatin sensitivity may lead to other conclusions. Thus, our study should primarily be regarded as a presentation of a methodological approach for investigating intratumoral heterogeneities in cisplatin distribution.

Acknowledgments

We wish to express our gratitude to Dr Johan Wennerberg for providing us with animals and tumors, to Dr Tommy Knöös for mastering the TMS, to Dr Harald Andersson for statistical assistance, all of them at the University Hospital of Lund. We also wish to thank Drs Leo den Engelse and Frank Blommaert at the Netherlands Cancer Institute, Amsterdam, for providing us with antibodies.

References

1. Vermorken JB, van der Vijgh WJF, Klein I, *et al.* Pharmacokinetics of free and total platinum species after short-term infusion of cisplatin. *Cancer Treat Rep* 1984; **68**: 505–13.
2. Terheggen PMAB, Floot BGJ, Scherer E, *et al.* Immunocytochemical detection of interaction products of *cis*-diammindichloroplatinum(II) and *cis*-diammine(1,1-cyclobutanedicarboxylato) platinum(II) with DNA in rodent tissues. *Cancer Res* 1987; **47**: 6719–25.
3. Johnsson A, Olsson C, Nygren O, *et al.* Pharmacokinetics and tissue distribution in nude mice: platinum levels and cisplatin–DNA adducts. *Cancer Chemother Pharmacol*, in press.
4. Andrews PA, Howell SB. Cellular pharmacology of cisplatin: perspectives on mechanism of acquired resistance. *Cancer Cells* 1990; **2**: 35–43.
5. Wennerberg J, Biörklund A, Tropé C. The effect of cisplatin and fluorouracil on xenografted human squamous cell carcinoma of the head and neck. *Arch Otolaryngol Head Neck Surg* 1988; **114**: 162–7.
6. Osieka R, Houchens DP, Goldin A, *et al.* Chemotherapy of human colon cancer xenografts in athymic nude mice. *Cancer* 1977; **40**: 2640–50.
7. Johnsson A, Olsson C, Andersson H, *et al.* Evaluation of a method for quantitative immunohistochemical analysis of cisplatin–DNA adducts in tissues from nude mice. *Cytometry* 1994; **17**: 142–50.
8. Sehested M, Hou-Jensen K. Factor VIII-related antigen as an endothelial cell marker in benign and malignant diseases. *Virchows Arch (Pathol Anat)* 1981; **391**: 217–25.
9. McCormick D, Chong H, Hobbs C, *et al.* Detection of the Ki-67 antigen in fixed and wax-embedded sections with the monoclonal antibody MIB 1. *Histopathology* 1993; **22**: 355–60.
10. Timmer-Bosscha H, Mulder NH, de Vries EGE. Modulation of *cis*-diamminedichloroplatinum(II) resistance: a review. *Br J Cancer* 1992; **66**: 227–38.
11. Deurloo MJM, Kop W, van Tellingen O, *et al.* Intratumoural administration of cisplatin in slow-release devices: II. Pharmacokinetics and intratumoural distribution. *Cancer Chemother Pharmacol* 1991; **27**: 347–53.
12. Richmond RC, Stafford JH, Ryan TP, *et al.* Platinum levels and clinical responses of tumours treated by cisplatin with and without concurrent hyperthermia: a case study. *Int J Hyperthermia* 1992; **8**: 147–56.
13. Bielack SS, Erttmann R, Looft G, *et al.* Platinum dispstition after intraarterial and intavenous infusion of cisplatin for osteosarcoma. *Cancer Chemother Pharmacol* 1989; **24**: 376–80.

(Received 24 August 1995; accepted 25 September 1995)